Coordination of Lead (II) and Cadmium (II) Ions to Nylon 6/flax Linum Composite as a Route of Removal of Heavy Metals

NT Moja

Institute for Nanotechnology and Water sustainability, College of Science, Engineering and Technology, University of South Africa

SB Mishra

Academy of Nanotechnology and Waste Water Innovations, Johannesburg, South Africa

SS Hwang

Department of Mechanical Engineering, Chien-Hsin University of Science and Technology, Chung-Li 32097 Taiwan, ROC

TY Tsai

Department of Chemistry, Master Program in Nanotechnology & Center for Nanotechnology, Chung Yuan Christian University, Chung-Li 32023, Taiwan, ROC

Ajay Kumar Mishra (ajaykmishraedu@gmail.com)

Research School of Polymeric Materials, School of Materials Science and Engineering, Jiangsu University, China https://orcid.org/0000-0002-3743-8669

Research Article

Keywords: Composite, Polymer, Metal, Adsorption, Aqueous solution

Posted Date: May 17th, 2021

DOI: https://doi.org/10.21203/rs.3.rs-521570/v1

Version of Record: A version of this preprint was published at Journal of Inorganic and Organometallic Polymers and Materials on June 18th, 2021. See the published version at https://doi.org/10.1007/s10904-021-02052-8.

Coordination of Lead (II) and Cadmium (II) ions to Nylon 6/Flax Linum composite as a route of removal of heavy metals

NT Moja[a], SB Mishra[b], SS Hwang[c], TY Tsai[d], AK Mishra[b,e,*]

[a]Institute for Nanotechnology and Water sustainability, College of Science, Engineering and Technology, University of South Africa
[b]Academy of Nanotechnology and Waste Water Innovations, Johannesburg, South Africa
[c]Department of Mechanical Engineering, Chien-Hsin University of Science and Technology, Chung-Li 32097 Taiwan, ROC
[d]Department of Chemistry, Master Program in Nanotechnology & Center for Nanotechnology, Chung Yuan Christian University, Chung-Li 32023, Taiwan, ROC
[e]Research School of Polymeric Materials, School of Materials Science and Engineering, Jiangsu University, China
Corresponding Author: ajaykmishra1@gmail.com

Abstract

Nylon 6 (PA6) reinforced Flax Linum composites were synthesized by melt mix extrusion and molded through Mucell\ ® injection technique for adsorption application for removal of Cd(II) and Pb(II) metal ions. The structural morphologies of all samples were evaluated using X-ray diffraction (XRD), Transmittance emission microscopy (TEM) and Scanning emission microscopy (SEM), indicating crystallized materials with pore-like cells and Thermographic analysis (TGA) illustrated the thermally stable., Microscopic PA6 revealed the effects of Flax content on both cell density and cell size of the foamed samples. The cell size of neat PA6 (48 μm) changed to 36, 17, and 15 μm after incorporation of Flax compositions for 1.0, 3.0 and 5.0 wt%. The removal of Cd(II)and Pb(II) with PA6/Flax 1.0 wt% composite was found to follow the Langmuir isotherm model. The results indicated that PA6 1.0 wt% composite can be efficiently used as a superabsorbent for the removal of Cd(II) and Pb(II) from aqueous solution.

Keywords: Composite, Polymer, Metal, Adsorption, Aqueous solution.

1. Introduction

Wastewater can be defined as spent or used water that has been discharged from industrial, domestic and agricultural activities and contains contaminants such as bacteria, heavy metals and fungi etc. Unlike most organic contaminants, heavy metals such as Nickel (Ni), Mercury (Hg), Lead (Pb) and Cadmium (Cd) are not biodegradable and tend to bio accumulate in living organisms [1]. These toxic metals are known to be mutagenic and carcinogens. Hence, when consumed over a long period of time, these cause severe illness such as heart failure, respiratory diseases, lung cancer, reproduction disorder and skin irritations, Therefore, out of the toxic metals that are found in the groundwater, Lead (Pb) and Cadmium (Cd) often exceeds the regulatory threshold limit set by WHO, US-EPA and SANS 241 wastewater, and thus pose a threat to the immediate environment and aquatic life [2]. Thereafter, it has become necessary to remove, remediate and minimize the concentration of these toxic metals in wastewater and water in general.

Wastewater, as is known, can be treated and purified by multiple techniques, such as desalination, filtration, membranes, flotation, adsorption, disinfection, sedimentation [3]. Certainly, adsorption has advantages over other methods in removal of heavy metals, such as ease of operation and comparatively low cost. Adsorption is the surface phenomenon whereby pollutants are adsorbed onto the surface of a material (adsorbent) via physical and/or chemical forces [4]. It depends on many factors or parameters such as temperature, solution pH, concentration of pollutants, contact time, particle size, temperature, nature of the adsorbate and adsorbent [5].

Coordination Polymers (CPs) are smart porous materials made from a variety of metallic substituents and suitable organic ligands. Researchers have recently attracted the phenomenon of incorporation of a metallic material in a matrix of a composite to enhance its performance. However, we have applied a polymer composite to adsorb Pb(II) and Cd(II). These material will

combine to form what is known as a copolymer. PA6 and Flax Linum has been combined to form a polymer composite. Over the past decades, synthetic polymers have been used as an adsorbent for the study of removal of toxic contaminants from wastewater [6]. Nylon 6 (PA6) or polyamide is one of the upcoming synthetic polymers in heavy metals remediation [7]. PA6 is derived from caproluctam. It is the major engineering and high performance thermoplastics class because of its good balance of material properties. Due to its repeating amide linkages such as –CO and NH–, and its swelling ability it is regarded as one of the best adsorbent for heavy metal ions [8]. In order to improve its chemical and reactive properties, PA6 can be modified using co-monomers such as Flax-Linum or stabilizers during polymerization to introduce new functional groups [9]. Recently, Flax-Linum materials emerged as promising adsorbents for the removal of heavy metals and organics because of their high specific surface areas [10]. In Flax family, Linum usitatissimum L. is a highly attractive material for adsorption of heavy metals from waste water. Flax and its derivatives have been examined for pollution management, for instance heavy metal adsorption [11]. The incorporation of Flax in nylon 6 polymer, increases its compressive strength, surface area, morphology and is biodegradable monolith [12]. The large-scale production of functionalized PA6 at low cost should result in good adsorbents for wastewater purification.

Hence, the development of novel polymer composite with increased affinity for removal of toxic metal ions .is desirable. Fortunately, Flax-Linum (modified)/PA6 composites are providing an opportunity to solve the above mentioned problem. PA6 is the most important polymer materials among synthetic polymers used as a matrix in polymer composites because of its superior properties such as excellent mechanical, thermal properties and high melting temperature [13]. These composites show considerable improvement in properties that cannot normally be achieved

using conventional composites or pure polymers. Among hybrid materials, the mixtures of synthetic and natural polymers represent a simple way to combine their best properties, obtaining materials with acceptable morphological, thermal, and mechanical properties, compared to pure polymers. Nonetheless, no studies have previously explored the possibility of using PA6/modified Flax-Linum for removal of Pb(II) and Cd(II). The aim of the present work is to develop, investigate and remediate Pb(II) and Cd(II) ions from aqueous solutions using nylon 6 incorporated with Flax-Linum

2. Materials and Method

2.1. Materials

Nylon or Polyamide 6 (PA6), 2100, with melt flow index 45 g/10 min and density 1.13 g/cm3 was supplied by Na-ya Plastics Co. Ltd, Taiwan. Flax without any pre-treatments was supply by a trading company with length of 2~3 cm and diameter of 10 μm (Figure 1).

2.2 Compounding and foaming process

The PA6/flax composites were prepared through the blending of Flax with PA6 resin using a twin-screw extruder. The loadings of Flax were 1 and 3 wt % respectively. Then, the composites were molded into dog-bone specimen separately using conventional and Mucell® injection molding processes. The Mucell® injection molding process was performed on a 100 ton ARBURG-420C injection molding machine, equipped with a microcellular foaming system. Nitrogen was used as a physical blowing agent in the foaming process. The processing parameters for both conventional and Mucell® moldings are presented in Table 1.

Table 1 Process parameters for PA6/Flax composite

Processing	Non-Foam	Foam
Melt Temp.(°C)	290	290
Mold Temp. (°C)	90	90
Injection Speed (cm^3/s)	140	150
Injection P.(Bar)	1000	700
V/P (cm^3)	3	1
Packing P.(Bar)	700-600	200
Packing Time (s)	5	0.5
Shot Size (cm^3)	22.5	17.5
Screw Speed (m/min)	25	25
Back P. (Bar)	50	110
Cooling Time (s)	25	25
SCF (s)	-	3

2.3 Characterization

The thermal decomposition temperature was determined by thermogravimetric analysis (TGA) (SII TG/DTA6200), and the experiment was performed by samples (10 mg) of air gas flow from 40 ºC to 900 ºC at a heating rate of 10 ºC min^{-1}. The dynamic mechanical analysis (DMA) was carried out with a TA-Q800 instrument with sample size: 35 mm * 12 mm * 3 mm in the air at a scanning range of 30–210 ºC with a heating rate of 5 ºC min^{-1}.. The dispersion morphology of PA6 composites was measured by scanning electron micrographs (SEM), Transmission electron microscopy (TEM), was obtained on a JEOL JSM 6500F, and Model JEOL JEM2010, 200 kV, respectively. 80 nm thickness of sample was prepared by using a Leica Ultracut-UCT to verify the physicochemical properties of layer materials. Thermogravimetric analysis (TGA) was carried out using SII TG/DTA6200, and the experiment was performed by a 10 mg sample of PP composites under air gas flow from 40 ºC to 900 ºC at a scanning rate of 10 ºC min^{-1}. The dynamic mechanical analysis (DMA) measurement was performed with a TA-Q800 instrument in the air at a scanning range of 30–210 ºC with a heating rate of 5 ºC min^{-1} with sample size: 35 mm * 12 mm * 3 mm. Tensile strength performed with Tensile Testing Machine Come tech D638 instrument. Analysis of metal trace was achieved by Inductive coupled plasma (ICP-OES) model 720 series.

2.4 Effect of variable parameters

2.4.1 Effect pH

The adsorption capacity of the PA6/Flax composites was determined by changing the pH of solution at a range of 2, 4, 6, 8, and 12 while the other parameters such as dose, temperature, time

and concentration were maintained and kept constant. The solutions used to control pH of the solution were 0.125 M HCl and 0.125 M NaOH for acidic and basic phase respectively.

2.4.2 Effect of initial concentration

The effect of the initial concentration of the model contaminants on the adsorption capacity of the PA6/Flax composite was studied by varying the initial concentrations of Pb(II) from 10, 20, 30, 40, and 50 ppm.

2.4.3 Effect of dose

In order to investigate the effect of adsorbent mass on the rate of adsorption 0.02g, 0.1g, 0.15g, and 0.2g of PA6/Flax composites masses were varied by mixing with aqueous solution in a mechanical shaker keeping the other parameters constant, such as pH at 6 for Pb(II) and 10 for Cd(II)), temperature (25˚C), contact time (30 min) and concentration at 10 and 20 mg/L respectively.

2.4.4 Effect of contact time

Time was also varied for adsorption capacity using PA6/Flax composites. Time range of 5, 15, 30, 45, 180, 240, and 1440 minutes were used. Other parameters such as pH (6 and 10 respectively), temperature (25), and concentration (10 and 20 mg/L respectively) were kept constant.

2.5 Batch equilibrium studies

A 100 ppm stock solution of Pb(II) and Cd(II) solution were prepared by dissolving lead nitrate $Pb(NO_3)_2$ and cadmium nitrate $Cd(NO_3)_2$ salts in de-ionized water. Batch adsorption experiments

were conducted to study the effect of pH, contact time and initial concentration and dose on Pb(II) adsorption. For all the experiments, adsorbent weight was fixed to be 0.050 g except on the studies on the effect of pH, and dosage where the weight was 0.150 g and the volume of Pb(II) solutions were fixed at 15 ml. Initial pH of the solution was adjusted using 0.125 M NaOH or HCl. The initial concentration range of 10 ppm to 50 mg/l was used. The solution was shaken thoroughly by a mechanical shaker rotating at 250 rpm, and filtered using a Whatsman filter paper at different time interval. After adsorption, the residual metal pollutant was determent by ICP-OES (Aligent 720 series)

The amount of metal adsorbed (qe) and percent of removal (%R) can be calculated using the following equations:

$$qe = \frac{(Co - Ce)}{Vm} \qquad (2)$$

$$\%R = \frac{(Co - Ce)}{Co} \times 100 \qquad (3)$$

Where qe is the amount of metal pollutant adsorbed (mg/g), Co and Ce are the initial and equilibrium concentrations of the metal pollutant, respectively. V is the volume of the solution in liters, and m is the weight of the polymer composite used in grams (g).

2.6 Batch kinetic studies

Kinetic experiments were identical to equilibrium experiments except for the variation of time. Further, the remaining concentration after adsorption was converted to adsorption capacity by:

$$qt = \frac{(Co - Ct)}{Ws} \qquad (4)$$

Where Ct is the remaining concentration (mg/l) at time (t). The other variables have the same meaning as in Eq. (3). The percent Pb(II) and Cd(II) removed. (R (%)) was calculated using Eq. (5).

$$\%R = \frac{(Co-Ct)}{Co} \times 100 \qquad (5)$$

3. Results & Discussion

3.1 Morphology of PA6 composites

PA6 composite morphology was confirmed using DMA, TGA, SEM, and TEM. Scanning electron microscope (SEM) was used to investigate surface morphology of PA6 and the effect of incorporation of Flax Linum polymer. Low and high magnification images of the neat and composite (reinforced with Flax) PA6 surfaces after modification are presented in Figure 1 below. SEM analysis at low magnifications showed neat PA6 indicated porous-like fracture and had rough surface after introduction of foaming agent, whilst composite (PA6/Flax) samples had rough, grainy surface indicating extensive deformation within the matrix complex, the distribution of Flax in PA6 matrix is clearly evident from hollow-like features that appear to be porous within the polymer matrix.

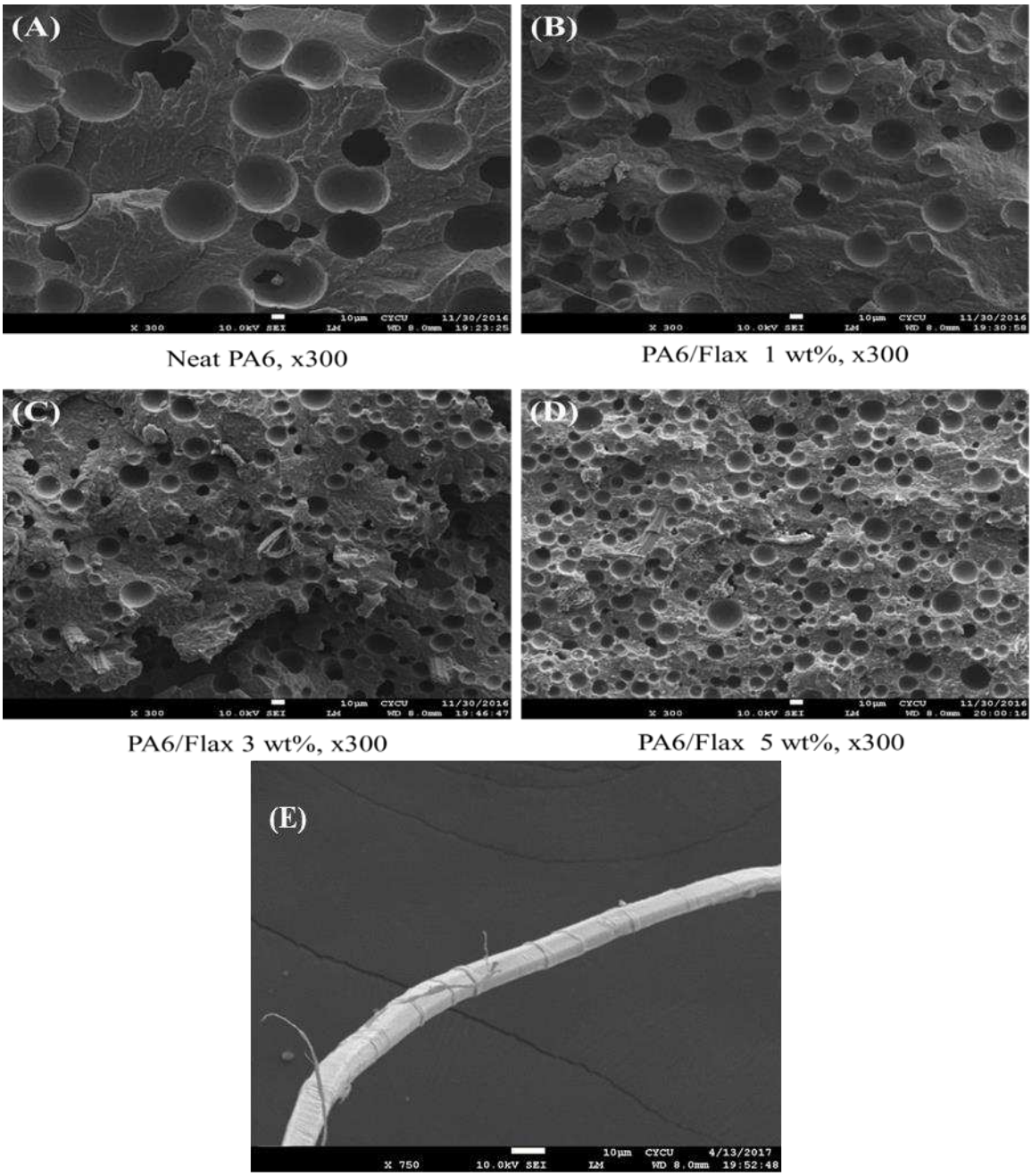

Neat PA6, x300

PA6/Flax 1 wt%, x300

PA6/Flax 3 wt%, x300

PA6/Flax 5 wt%, x300

Neat Flax, ×10μm

Figure 1: SEM images of PA6/Flax nanocomposit

3.2 Mechanical Properties of PA6 Composites.

The storage modulus versus temperature curve reflects the whole tensile development of the elastomeric composites which will assist us in understanding the engineering application PA6/Flax Linum. Figure 2a illustrates the stress–strain behavior of neat PA6 and PA6/Flax Linum composites. From Fig. 2a it is evident that the stress–strain characteristics for all composites are quite different. As the concentration of Flax Linum increases in the PA6/Flax complex. The composite with PA6/Flax 5 wt % has the highest stress value in the early stages of the strain development and the stress doesn't change in plastic region. This behavior (for PA6/Flax 5 wt %) indicates a highly toughness of the material therefore having a higher fracture energy. The stress value for neat PA6 shows increasing trend in the early stage of the strain development while the stress increases with slow rate in the plastic region. The storage modulus can exhibit the stiffness of the material. The storage modulus is 2399, 2622, 2775, 3221 MPa at 60°C for the neat PA6 1, 3, 5 wt% Flax, respectively. In fig. 2b the glassy state is not present but illustrates a rubbery plateau for all materials. As the Flax Linum content in the PA6/flax Linum matrix increases, the young's modulus increases however, as the temperature increases there's an abrupt change indicating deformation in the structure. From a rubbery plateau (Tg) to fluid (Tm).

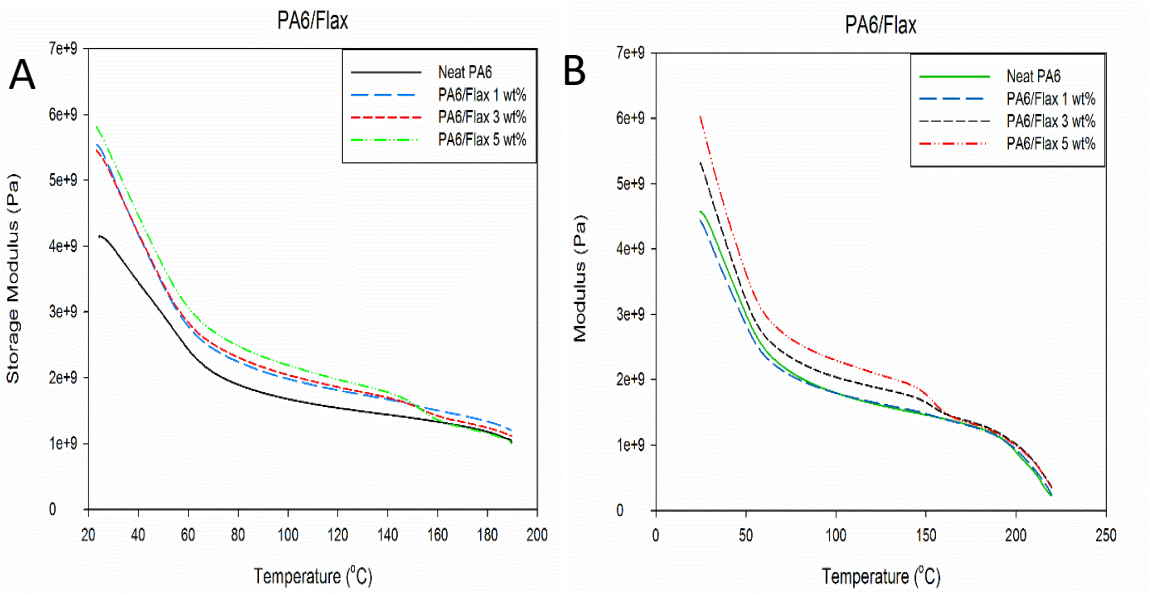

Figures 2 a.) Shows the storage modulus vs temperature and b is modulus Vs temperature of neat PA6 and PA6/Flax Linum composites

3.3 Thermal properties of PA6 Composites

DSC measurements were carried out to analyse the thermal transitions and crystallinity of PA6 and PA6/Flax Linum composite. DSC curves of the samples for melting and crystallization are shown in Fig. 3. The related crystallization temperature (Tc) and melting temperature (Tm) are summarized in Table 2. In the graph, it is illustrated that Tm of PA6/flax Linum decreased as the content of Flax Linum increased. This phenomenon was due to the symmetry and regularity of PA6 chain that was destroyed during the formation of the complex. In the crystallization curves, the value of Tc was also found to shift to lower temperature with an increase in the content of DDP. This could be attributed to the deformation of PA6 during complex formation, which restrained PA6/Flax Linum to crystallize at high temperatures [14].

Table 2. Thermo-mechanical properties of PA6 composites

Sample	T_d (°C)	Tcc (°C)	ΔH (J/g)	Tm (°C)	ΔH (J/g)	Crystallinity (%)
PA6	470 ± 0.3	182.62	47.57	222.49	36.71	5.72%
PA6+Flax 1 wt%	468 ± 0.5	183.97	62.86	221.66	53.48	4.96%
PA6+Flax 3 wt %	469 ± 0.1	183.61	61.27	221.89	50.16	5.91%
PA6+Flax 5 wt %	471 ± 0.2	184.16	55.78	222.05	48.05	4.19%

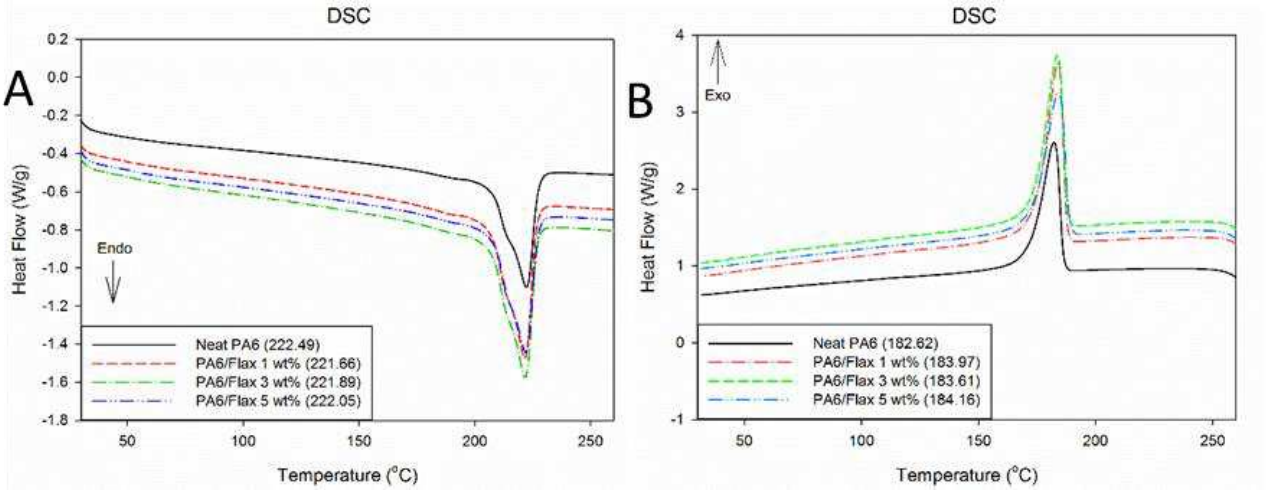

Fig. 3 DSC curves of PA6 and PA6/Flax Linum for crystallization (a) and melting (b)

The TGA results of the composites are as shown in Fig 4. 4a shows the thermgravemetric analysis whereas 4b represents differential thermo-gravimetric analysis. The thermal stability of the PA6/Flax composites and the thermal decomposition temperature (T_d) were increased as compared to that of the neat polymer, while the thermal decomposition temperature decreased for PA6. This is caused by the good interface bonding between the Flax and the PA6 in the complex matrix. Fig. 4b indicates DTG curves, which shows small peaks at about 200 ◦C, which can be associated with deformation an amide functional group in PA6/Flax Linum complex. In the second stage, within the range of 370–530 ◦C, a decline derived from the thermal decomposition of ketone functional group.

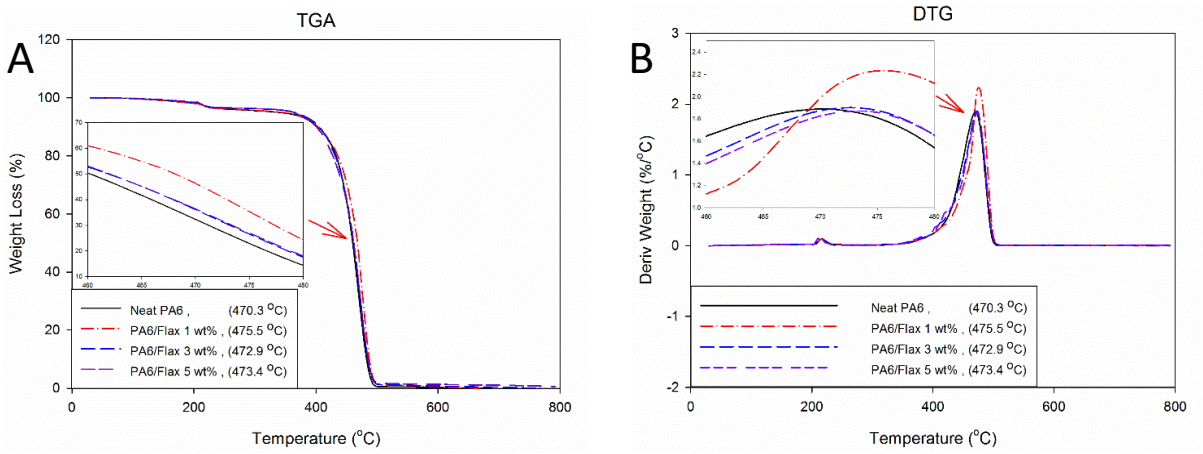

Figure 4: a) TGA curve and b) DTG analysis of PA6/Flax

In order to evaluate the effect of PA6/Flax Linum on the foaming behavior from PA6 polymer, the cell size and cell densities of the prepared PA6 and PA6/Flax Linum foams are summarized in Fig. 5. It can be observed that cell size reduces gradually and cell density increases gradually, with an

increase in the Flax Linum granule content. Remarkably, as Flax Linum content reaches 5 wt%, the cell size is decreased to numerous hundred nanometers, and the cell density is increased to 4.8 × 10^{13} cells/cm^3. Compared with the pure PA6 foam, the cell density of PA6/Flax Linum 5 wt% composite foam is increased by nearly two folds of amount [15]. All these phenomena demonstrate that the Flax granules are very effective heterogeneous nucleating agents in promoting cell nucleation of PA6 during the microcellular foaming. The pronounced effect of Flax Linum in enhancing cell nucleation can be attributed to an addition of Flax Linum which generates a large number of heterogeneous interfaces and reduces cell nucleation energy [16]

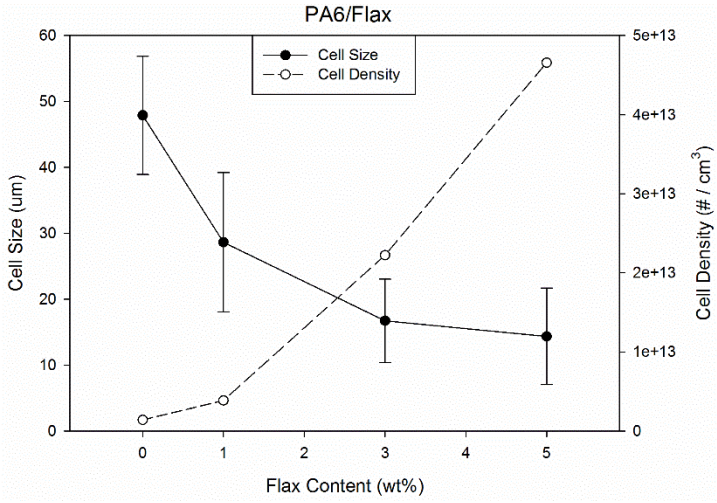

Figure5: illustration of impact of flax on PA6 cell size and density

3.4 Adsorption studies

3.4.1 Adsorption experiments

The batch adsorption experiments were carried out with 0.2 g of PA6-Flax Linum- and 15 mL of Cd (II) and Pb (II) aqueous solutions with the standard concentration and appropriate pH. The pH

values of the suspensions were adjusted with 0.1 mol/L HCl and NaOH. Then, the suspensions were shaken for 30 min to achieve adsorption equilibration. The suspensions were filtered with universal sieve and the concentrations of metal ions in the filtrate were determined using ICP-OES 720 series. The amount of metal ions adsorbed on PA6-Flax Linum (mg/g) was calculated from the difference between the initial concentration Co (mg/L) in aqueous solution and the equilibrium concentration Ce (mg/L) determined in solution after filtration: qe =(Co-Ce)V/m adsorbent, where V is the volume of the suspension, and adsorbent is the mass of PA6-Flax Linum.

In order to confirm the chemical nature of adsorption, the relative isotherms were applied to measurements of the performance of PA6-Flax Linum before and after adsorption of metal. The kinetic experiments were identical to equilibrium experiments except for the variation of time. Further, the remaining concentration after adsorption was converted to adsorption capacity by:

$$qt = \frac{(Co - Ct)}{Ws} \qquad (4)$$

Where Ct is the remaining concentration (mg/l) at time (t). The other variables have the same meaning as in Eq. (3). The percent Pb(II) removed. (R (%)) was calculated using Eq. (5).

$$\%R = \frac{(Co - Ct)}{Co} \times 100 \qquad (5)$$

3.4.2 Mechanism

Diagram 1 below shows the possible bonding mechanism between the PA6 and Flax composite with Pb (II). As illustrated below, PA6 is modified with Flax, through covalent bonding. As a result a composite is formed with improved characteristics for adsorption of Cd(II) and Pb (II)

ions. PA6 has N-H, and it is highly porous while Flax has excess OH^- functional groups, hence a good combination for adsorption processes. At pH 6 the adsorption of Pb (II) reaches optimal, and Cd(II) reached optimal at pH10, this may be due to the increase of OH^- (hydroxyl ions).Therefore, the sudden increase of Pb (II) at pH < 7 is not attributed to the formation of $Pb(OH)_2$. In conclusion, the results in Figure 7, indicate that the best pH values of the binary system to remove Pb(II) from solution by using PA6/Flax 1 wt%, similarly with Cd(II)

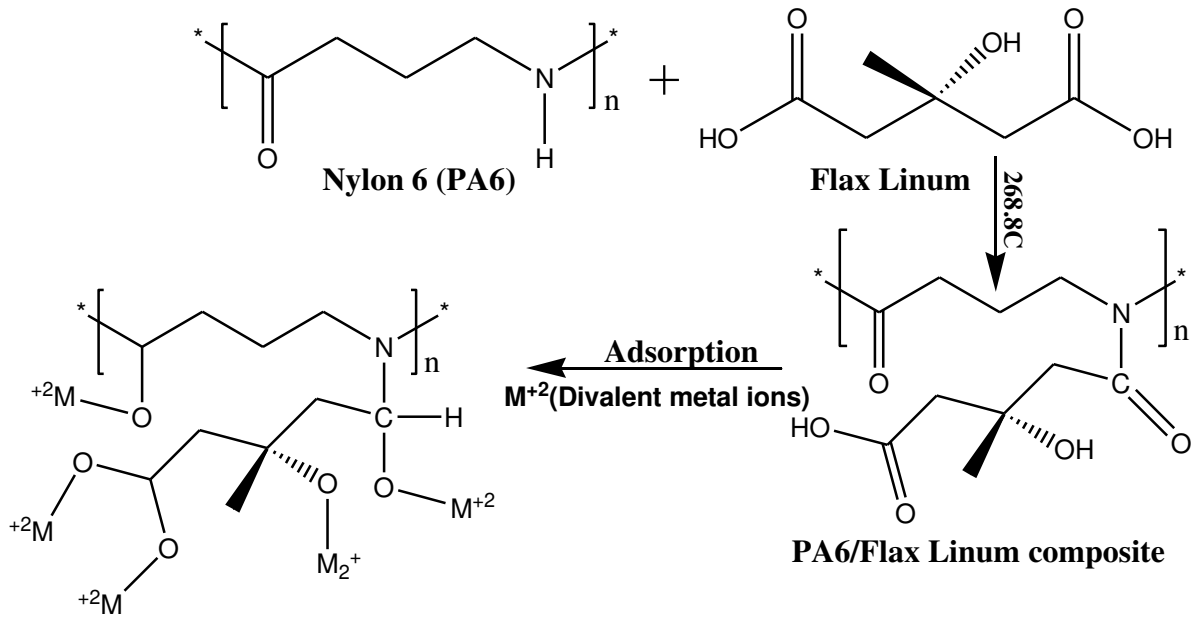

Diagram 1: Mechanism illustrating the removal of Pb (II) and Cd (II)

3.5 Heavy metal uptake (Kinetics)

3.5 **Effect of concentration**

Figure 6 below illustrates the effect of initial concentration of Pb(II) and Cd(II). There were five different initial concentrations of both Pb(II) and Cd(II) chosen for the study i.e. 10, 20, 30, 40 and 50 mg/l with a constant dose of 0.5 g of adsorbent composite. From the figure below, it is observed

that PA6-Flax wt 1% is the most efficient adsorbent for adsorption of Pb(II) and Cd(II). In both incidence, PA6-Flax wt 1% has <75% adsorption efficiency at concentration 10 and 20 mg/L respectively. The ability of PA6-Flax to adsorb Pb(II) and Cd(II) is attributed to the presence of ions, such as OH^-, O^-, N-H and the swelling ability. PA6-Flax wt 1% polymer composite was able to adsorb almost 76.03% of Cd(II) at 20 mg/l and Pb(II) with 87.40 % removal at 10 mg/l using 0.5g dosage in both cases . Fig 6A: Explain why PA6-Flax wt1% shows abrupt values and the reoval of 75% when compare to the rest of the composites where as in 6B it does not show any indifferent. How concentration of Cd and Pb does has an effect on the adsorption?

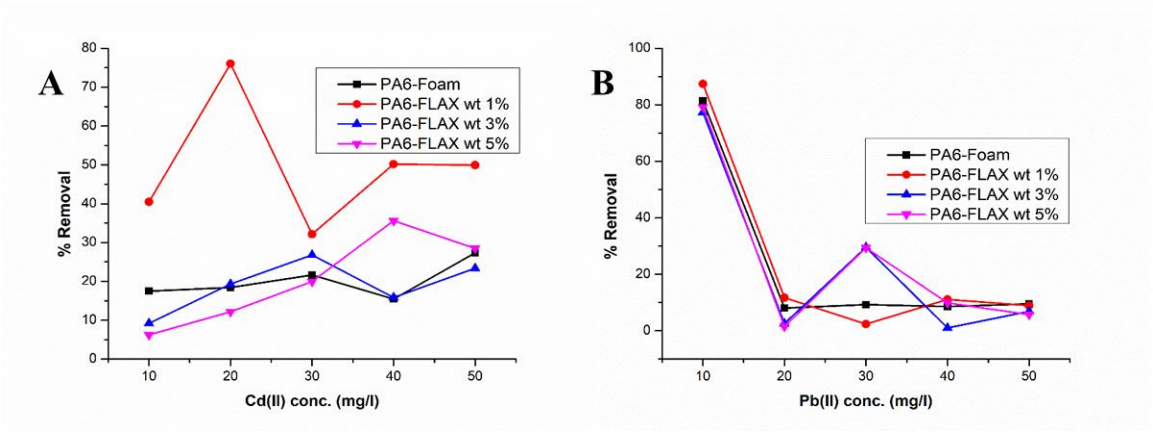

Figure 6: Effect of initial concentration for adsorption Cd(II) [A] and Pb(II) [B] using PA6-Flax Linum composite (0.5g dosage of PA6, PA6-Flax Linum Wt%)

3.6 **Effect of pH**

Metal ions in water solution can be presented in different forms at various pH values [17]:

$$Me^{2+} \leftrightarrow Me(OH)+ \leftrightarrow Me(OH)2 \leftrightarrow Me(OH)3$$

Where Me represents metal ions

As a result, pH of a solution is an important factor in adsorption of metal ions on PA6-Flax Linum. The adsorption of metal ions on PA6-Flax Linum was investigated at various pH, ranging from 2 to 12. As shown in Fig. 7 below, the adsorption of Cd(II) increases drastically from pH 2–10 and shows a sudden drop in the efficiency removal from pH 10–12. At pH 10 the predominant cadmium species is Cd^{2+} (>95.30%). Moreover, the pHpzc (point of zero charge) value of PA6 is at pH 5.2–5.5, Therefore, at pH > 5.5 (pH > pHpzc), the surface charge of PA6 is negative and the electrostatic interactions between the metal ions and PA6 become stronger [18]. In the case of Pb(ii), the high adsorption is also observed in acidic solution, i.e. 99.34% of metal ions are removed from the solution at pH = 6. The adsorption of Pb(ii) increases at pH 2–6, and drops at pH 6–8 (the predominant lead specie is Pb^{2+} with >99.34%). From pH 8–10 there is a gradual increase in removal of Pb^{2+} ions. A pH higher than 5 is favorable for the ionization of the oxygen-containing functional groups on the surface of PA6-Flax Linum that play a significant role in the uptake of metal ions. The negative charges generated on the PA6-Flax Linum surface enlarged the cation-exchange capacity of PA6-Flax Linum and, simultaneously, the electrostatic attraction became more important. The adsorption of metal ions decreases at lower pH due to the low dissociation of the functional groups and competition between H^+ and metal ions for the same sorption site. The slight decrease of adsorption Pb(II) at pH 6–8 can be explained by the formation of hydroxide complexes $Pb(OH)^+$. At pH from 6 to 8, the relative concentration of $Pb(OH)^+$ increases from ca. 5 to 55% [19]. The positive charge of hydroxide complexes is lower than Pb^{2+} and the electrostatic attraction slightly decreases. As shown in Fig. 3, the metal ions begin to form a precipitate at different pH values depending on initial metal concentration (the solubility products pKSP of $Cd(OH)^{2+}$ and $Pb(OH)^{2+}$ are 14.14, 14.84, respectively) Taking into consideration the

high adsorption of metal ions from aqueous solution (pH from 4 to 8) and to prevent precipitation of metal hydroxides.

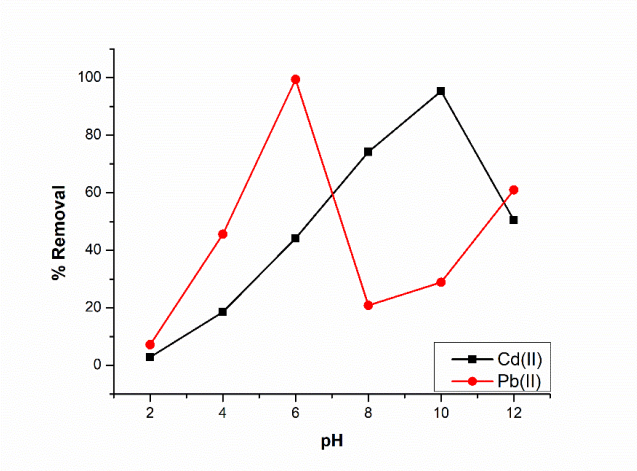

Figure 7: Effect of pH for adsorption Cd(II) and Pb(II) at optimum concentration (20, 10 respectively) using PA6-Flax Linum composite

3.7 **Effect of dose and contact time**

The adsorbent dosage is an important parameter for adsorption for kinetics efficiency during treatment at a wastewater treatment. Figure 8a illustrate removal efficiency over a variation of dose (0.1 to 0.6g). The figure clearly shows that the removal efficiency of Cd(II) and Pb(II) reached optimal at 92% and 72% respectively with 0.2g [20]. However, the removal of Pb(II) illustrates that with increasing of the adsorbent dosage there's a significant change which is attributed to the availability of a larger surface area and more adsorption sites. Similarly with Cd(II). However, Cd(II) shows a minor drop of percentage removal, the sudden drop at 0.3 g is attributed to a cluster of competing ions available in the composite. The effect of contact time on remediation of metal ions by PA6-Flax Linum 1 wt% is shown in Fig 8b below. Moreover, the kinetic curve illustrated

that the adsorption of Cd(II) and Pb(II) was fast and reached equilibrium after 30 and 90 min of contact respectively. The rapid adsorption can be more clarified by the availability of active sites from the Flax Linum with excess OH^- functional groups. The rate of removal of Cd(II) showed higher capacity, with 1004 mg/g in 30 min and consequently Pb(II) illustrates 599 mg/g rate of removal within 90 min. We also note that the adsorption affinity depends on a number of factors such as the nature, charge and size of metal ions, and the affinity of donor atoms towards each metal. Hence, it's not unexpected to have different affinities and adsorption efficiency and capacity using the same adsorbent with respect to different metal ions

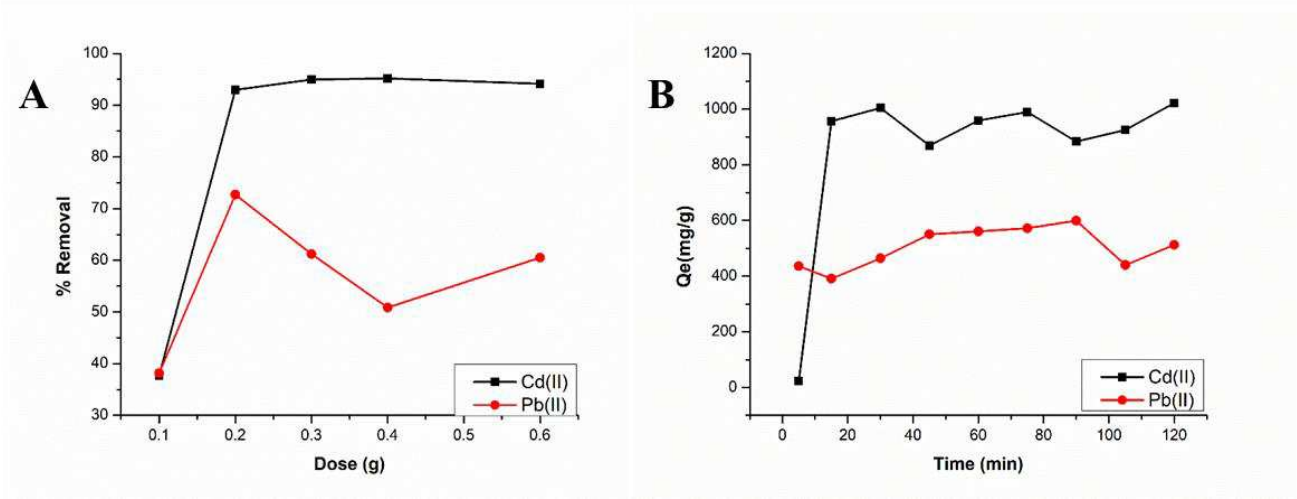

Figure 8: a.) Effect of dosage for adsorption Cd (II) and Pb (II) using PA6-Flax Linum composite and b.) : Effect of time in capacity adsorption for remediation Cd(II) and Pb(II) using PA6-Flax Linum wt 1% composite

3.8 Adsorption isotherms

Adsorption isotherm gives the different curves which describes the main phenomena of the retention of constituent from the water environment to a solid phase at constant pH and temperature. Isotherms are very important as they describe the interaction between adsorbate and adsorbent. Adsorption isotherms help to find out the relationship between amount of adsorbate adsorbed on the adsorbent and the left out concentration of adsorbate in liquid at the time of equilibrium.

3.9 Langmuir isotherm model

Langmuir isotherm model generally describes gas-solid phase adsorption. This empirical model assumes monolayer adsorption, where adsorption can only occur at definite localized sites [21]. Derivation of Langmuir isotherm represents the homogenous adsorption, where each molecule possesses constant enthalpies and sorption activation energy. It is characterized by plateau, an equilibrium saturation point. It can be represented as:

$$\frac{1}{qe} = \frac{1}{Q°K} + \frac{1}{KQ°Ce} \qquad (1)$$

Where C_e is the metal concentration at equilibrium. Langmuir constant (dm^3/g) is represented as K. Q_{max} is the monolayer capacity of the synthesized sample (mg/g). The constants K_L and Q_{max} were calculated from the intercept and slope of the linear plot of $1/Q_e$ and $1/C_e$ (Fig. 10) and the results are given in Table 3.

In this study, a plot of Ce/qe against Ce produces a straight line with a correlation coefficient (R^2=1) for both Cd(II) and Pb(II), indicating that the adsorption of the pollutant on PA6/Flax 1% wt polymer composite follows Langmuir isotherm [22] as given in Figure 10A. Furthermore, the separation factor RL of Cd(II) and Pb(II) defined by Eq. 7, was calculated from Langmuir isotherm parameters and was found to be 0.01 and 0.006 respectively

$$\mathrm{RL} = \frac{1}{1+\mathrm{K}Co} \qquad (2)$$

Where Co is the optimum initial concentration (mg/L) of metal ions and K is related to the energy of adsorption (L/mg)

3.10 Freundlich Isotherm

Considering the Freundlich isotherm model, the logarithmic form of the equation was applied, given by eq. (3) below:

$$qe=KfCe^{1/n} \qquad (3)$$

Logarithmically equation (3) above can be transformed to Eq. (4):

$$\log qe = \log \mathrm{K}f + \frac{1}{n}\log Ce \qquad (4)$$

Where Kf and n are the Freundlich constants. A plot of log Ce vs. log qe (Fig. 10 B) yields a linear curve with the intercept value of Kf and the slope of n. Kf Value shows the adsorption capacity of the adsorbent [22] as; the slope $1/n$ specifies adsorption intensity. Freundlich isotherm model is commonly used but does not provide much information on the monolayer adsorption capacity in contrast to the Langmuir model. In this study, the plot of log Ce against log qe was

employed to obtain from the intercept the value of K_f and from the slope the value of n. Figure 13b, the Freundlich constants K_f and n were found to be 2.72 mg/g for Cd(II) and 2.78 mg/g for Pb(II). The isotherm data does not fit the Freundlich model well on both incidences ($R^2 = 0.978$). Hence, it does not favor good adsorption. The Non-linear plot indicates that the adsorption of Pb (II) and Cd(II) ions onto polymer composites does not follow the Freundlich isotherm. Also, the slope 1/n indicates the effect of concentration on the adsorption capacity and represents adsorption intensity all sorption measurement are illustrated in Table 3 below.

3.11 Temkins Isotherm

In Figure 10 C Temkin Isotherm is shown. The Temkin isotherm is usually used for heterogeneous surface energy systems (non-uniform distribution of sorption heat). In addition; containing a factor, explicitly taking into the account of adsorbent–adsorbate interactions [22] as. By overlooking the amount of concentrations, the model assumes that heat of adsorption ΔH (as a function of T in kelvin) of all particles in the layer would reduce linearly rather than logarithmic with coverage. As described in the equation below; its derivation is measured by a uniform distribution of binding energies (up to some maximum binding energy) was carried out by plotting the quantity adsorbed qe against ln Ce and the constants were determined from the slope and intercept. The model is given by the following equation below; where AT is Temkin isotherm equilibrium binding constant measured in L/g, Bt are Temkin isotherm constant, R is universal gas constant (8.314J/mol/K), T is Temperature at 298K and lastly B is constant related to heat of sorption(J/mol)

$$qe = \frac{\mathrm{RT}}{\mathrm{B}} \ln \mathrm{K}tCo \qquad (5)$$

The linearized equation (5) above can be transformed to Eq… (6) below

$$qe = \frac{\mathrm{RT}}{\mathrm{B}}\ln \mathrm{K}t + \frac{\mathrm{RT}}{\mathrm{B}}\ln Ce \qquad (6)$$

From the plot in Fig 10C, Temkins calculations are estimated; where: A_T = 1.075 L/g, B_T= 25.34 J/mol which is an indication of the heat of sorption indicating a physical adsorption process and the **R^2=0.9387.**

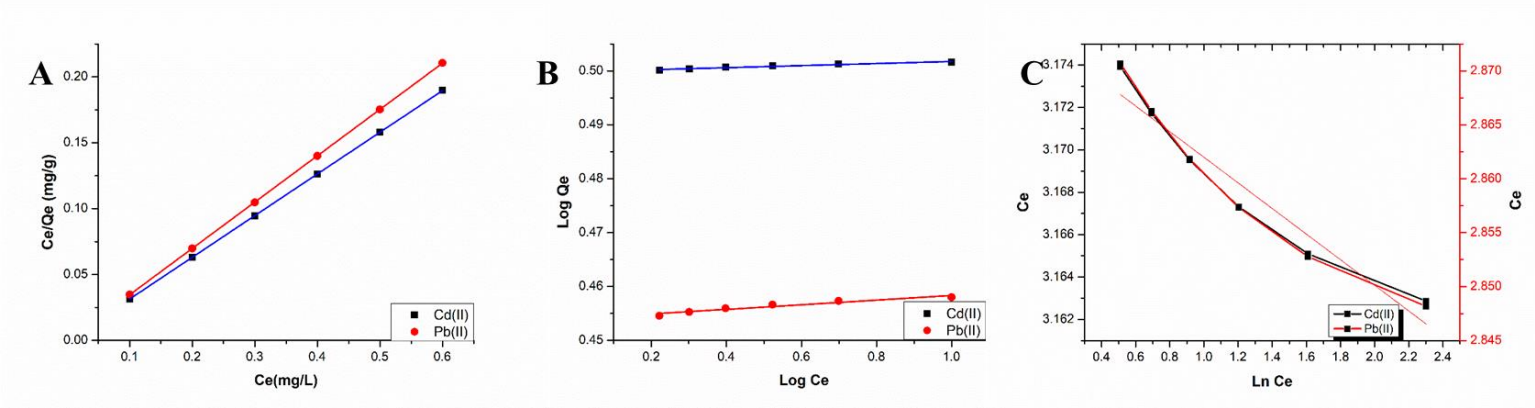

Figure10: Linearized fits for Langmuir isotherm 10 mg/l of Pb(II) and 20 mg/l of Cd(II) of by PA6/Flax 1wt% , **b)** Linearized fits for Freundlich isotherm 10 mg/l of Pb (II) and 20 mg/l of Cd(II), of PA6/Flax 1wt% composite, **C)** Linearized fits for Temkins isotherm 10 mg/l of Pb (II) and 20 mg/l of Cd(II), of PA6/Flax 1wt% composite

Table 3: Langmuir model, Freundlich, Temkins model results of PA6-Flax Linum composites

	Langmuir Isotherm			**Freundlich Isotherm**			**Temkins Isotherm**		
Metal ions	RL	K	R^2	K_f	N	R^2	b_T	A_T	R^2
Cd(II)	0.01	5.7	1	2.72	5.26	0.9343	97.82	1.075	0.938
Pb(II)	0.006	15.8	1	2.78	2.32	0.9321	97.82	1.075	0.980

3.12 Kinetic modeling

3.12.1 Kinetic study

The time which metal ions and the adsorbent are in contact is an essential matter in the removal of contaminants from the environment in the process of adsorption. Fig. 11 shows the adsorption of metal ions, which increases exponentially at the beginning of the investigation and then reached equilibrium in a short time. The time required to reach equilibrium depends on metal ions to be adsorbed. The percentage of adsorption reached above 90% after 10, 15 min for Cd(II) and Pb(II), respectively. Adsorption at 99% level can be obtained after 30 min for both Cd(II) and Pb(II).The correlation coefficients for the second-order kinetic model are greater than 0.9 indicating the applicability of this kinetic equation and the second-order nature of the adsorption process of Cd(II) and Pb(II) ions onto PA6/Flax 1%wt polymer composite. If the 2nd order kinetics is applicable, the plot of t/q(t) versus t should shows a linear relationship. Fig.11 shows the plot for pseudo-2nd order model. The linear fit with correlation coefficient, R^2 = 0.9645 for Cd(II) and R^2 = 0.9555 for Pb(II) which illustrates that the adsorption follows the pseudo-second-order model on both occasion.

The kinetics of an adsorption process was studied using the pseudo-first and pseudo-second-order rate adsorption kinetic models. These models can be expressed as follows:

$$\log(qe - qt) = logqe\frac{Kad}{2.303}t \quad \text{And} \quad \frac{t}{qt} = \frac{1}{K2qe^2} + \frac{t}{qe} \qquad (7)$$

Where qe and qt (mg/g) are the capacities of Cd(ii) and Pb(ii), adsorbed at equilibrium and time t (min), respectively, k1 is the pseudo-first-order rate constant (min^{-1}), and k2 is the pseudo-second-order rate constant (g m/(g min)).

Kinetics of adsorption process may also be analyzed by pseudo second-order rate equation [23] as. The pseudo-second-order model is based on the assumption that biosorption follows a second-order mechanism, whereby the rate of sorption is proportional to the square of the number of unoccupied sites. The linearized form of the equation is expressed as:

$\frac{tq}{t¼}(K2ads)\frac{qe2}{tqe}$ (8)

Where K_2 ads is the rate constant of second-order bio sorption (g/m eq min).

The linearized second-order plot of t/q against t

According to Eq. (8) resulted in straight lines for Cd, and Pb ions led to the determination of the second-order rate constants k_2,ads and qe from the slope and they-intercept . The qe values were very close to the experimentally determined ones, a first sign of the appropriateness of this model. The R_2 values for the second-order kinetic model were 1 for the adsorption of Cd and Pb ions onto

modified nylon. This results correlates with Schiewer and Patil, who showed that bio-sorption of divalent metals by protonated pectin peels was fitted a second-order model better than a first-order model.

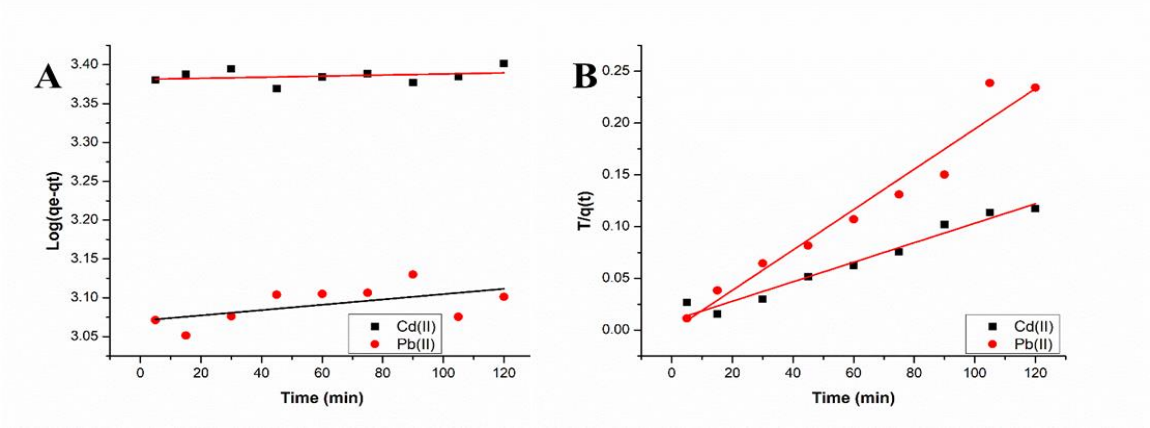

Figure 11: Linearized fits for pseudo 1st order (A) of PA6/Flax, Linearized fits for 2nd order (B) of PA6/Flax composite

4. Conclusions:

Instrumental analysis of PA6/Flax composites performed illustrates a successfully synthetic route of…injection molding for fabrication of modified composites. Increased crystallinity of 1 wt% and 3 wt% of the composite magnifications showed neat PA6 experienced porous-like fracture and had rough surface after introduction of foaming agent, whilst composite (PA6/Flax) samples had rough, grainy surface indicating extensive deformation within the matrix complex, the distribution of Flax in PA6 matrix is clearly evident from hollow-like features that appear to be porous within the polymer matrix using SEM analysis. Neat PA6 and synthesized PA6/Flax composite obtained with ratio 1, 3, 5 wt% were used for heavy metal adsorbent for adsorption of Cd(II) and Pb(II) from aqueous

solutions. The rate of removal of Cd(II) showed higher capacity, with 1004 mg/g in 30 min and consequently Pb(II) illustrates 599 mg/g rate of removal within 90 min, with <95% pollutant removal for both metal ions.The removal of Cd(II) and Pb(II) with PA6/Flax 1 wt% composites were found to follow the Langmuir isotherm. Pb(II) ions were adsorbed on homogeneous sites whose binding energies were uniform and consequently made a layer on the surface of the composite. It has been established that the removal of Cd(II) and Pb(II) from aqueous solution is predominantly through chemical adsorption due to pseudo-second order kinetics.

Acknowledgements

Authors are thanks to the National Research Foundation (NRF), South Africa and Ministry of Science and Technology (MOST), Taiwan for the financial support.

References

[1] S. Ponnusamy and S. Anbalagan, "Sustainable wastewater treatments in textile sector," *Sustainable Fibres and Textiles,* vol. 2017, pp. 323-346, 2017.

[2] H. Ali, E. Khan and I. Ilahi, "Environmental chemistry and ecotoxicology of hazardous heavy metals: Environmental persistence, toxicity, and bioaccumulation," *Journal Of Chemisry,* vol. 2019, pp. 1-14, 2019.

[3] S. Sharma and A. Battacharya, "Drinking water contamination and treatment techniques," *Applied Water Science ,* vol. 7, p. 1043–1067, 2017.

[4] Y. Wang, C. Pan, W. Chu, V. A.K. and L. Sun, "Environmental remediation applications of carbon nanotubes and graphene oxide: adsorption and catalysis," *Nanomaterials ,* vol. 9, no. 3, p. 439, 2019 .

[5] S. Banerjee and M. Chattopadhyaya, "Adsorption characteristics for the removal of a toxic dye, tartrazine from aqueous solutions by a low cost agricultural by-product," *Arabian Journal of Chemistry,* vol. 10, no. 2, pp. 1629-1638, 2017.

[6] B. Urbano, S. Bustamante, D. Palacio, M. Vera and B. Rivas, "Polymer supports for the removal and degradation of hazardous organic pollutants: an overview," *Polymer International,* vol. 69, no. 4, pp. 333-345, 2019.

[7] M. Shalaby, H. Abdallah, A. El-Gendi and S. Ali, "Microfiltration/ultrafiltration polyamide-6 membranes for copper removal from aqueous solutions," *MembraneWater Treatment,* vol. 7, no. 1, pp. 55-70, 2016.

[8] J. Ruiz, M. Trigo-López, F. García and J. García, "Functional aromatic polyamides," *Polymers,* vol. 9, no. 414, pp. 1-44, 2017.

[9] O. Kyunghwan, K. Hoyeon and Y. Seo, "Effect of diamine addition on tructural features and physical properties of polyamide 6 synthesized by anionic ring-opening polymerization of ε-caprolactam," *Journal Of ACS Omega,* vol. 4, no. 17, p. 17117–17124. , 2019.

[10] G. Kyzas, E. Christodoulou and D. Bikiaris, "Basic dye removal with sorption onto low-cost natural textile fibers," *Journal Of Processes,* vol. 1, no. 166, pp. 1-18, 2018.

[11] A. Jamshed, A. Hamid, N. Muhammad, A. Naseer, M. Ghauri, J. Iqbal, S. Rafiq and N. Shah, "Cellulose-based materials for the removal of heavy metals from wastewater – An overview," *Jounal Of ChemBioEng Reviews,* vol. 4, no. 4, p. 1–18, 2017.

[12] J. Cho and J. Cho, " Nylon 6 nanocomposites by melt compounding," *Polymer,* vol. 42, pp. 1083-1094, 2001.

[13] D. Battacharyya, "Polyamide 6 single polymer composites," *eXPRESS Polymer Letters,* vol. 3, no. 8, pp. 525-532, 2009.

[14] M.-W. H. J.-J. Shao, Y.-X. Chen and H. S-S., "Synthesis and characterization of the microcellular injection molded PA6/flax and the PA6/graphene nanocomposites," *Materials Science and Engineering542 (2019) ,* vol. 542, pp. 1-11, 2019.

[15] A. Bergeret and J. Beneze, "Natural fibre-reinforced biofoams," *International journal of polymer science,* vol. 2011, pp. 1-14, 2011.

[16] A. Goyal, V. Sharma, N. Upadhyay, S. Gill and M. Sihag, "Flax and flaxseed oil: an ancient medicine & modern functional food," *J Food Sci Technol. ,* vol. 51, no. 9, p. 1633–1653. , 2014.

[17] R. Sitko, E. Turek, B. Zawisza, E. Malicka, E. Talik, J. Heimann, A. Gagor, B. Feista and R. Wrzalik, "Adsorption of divalent metal ions from aqueous solutions using graphene oxide," *Journal of Dalta Transaction,* no. 16, pp. 1-17, 2013.

[18] V. Leone, M. Pereira, S. Aquino, L. Oliveira, S. Corrêa, T. Ramalho, L. Gurgel and A. Silva, "Adsorption of diclofenac on a magnetic adsorbent based on maghemite: Experimental and theoretical studies," *New Journal Of Chemistry,* vol. 42, no. 1, pp. 1-25, 2017.

[19] E. Turek, B. Zawisza, E. Malicka and R. Sitko, "Adsorption of divalent metal ions from aqueous solutions using graphene oxide," *Journal Of Dalton Transactions,* vol. 16, p. 42, 2013.

[20] T. Naiya, A. Bhattacharya and S. Das, "Removal of Cd(II) from aqueous solutions using clarified sludge," *Journal of Colloid and Interface Science,* vol. 325, no. 1, pp. 48-56, 2008.

[21] A. Ebelegi, D. Wankasi and N. Ayawei, "Modelling and Interpretation of Adsorption Isotherms," *Journal Of Chemistry,* vol. 2017, pp. 1-12, 2017.

[22] N. Ayawei, A. Ebelegi and D. Wankasi, "Modelling and interpretation of adsorption isotherms," *Journal Of Chemistry,* vol. 2017, pp. 1-12, 2017.

[23] M. Athar, U. Farooq, M. Aslam and M. Salman, "Adsorption of Pb(II) ions onto biomass from Trifolium resupinatum: equilibrium and kinetic studies," *Journal Of Applied Water Science,* vol. 3, p. 665–672, 2013.

Figures

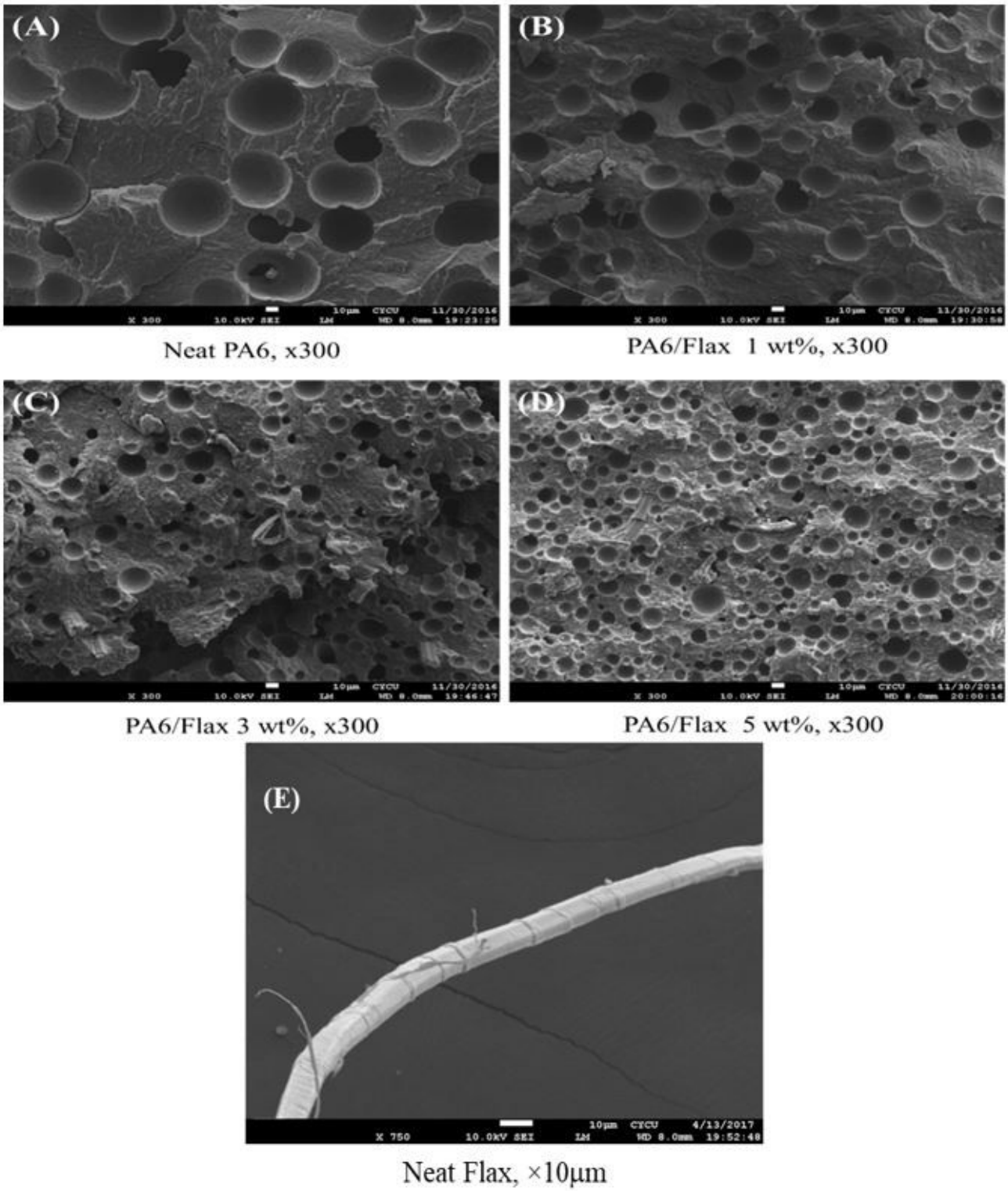

Figure 1

SEM images of PA6/Flax nanocomposit

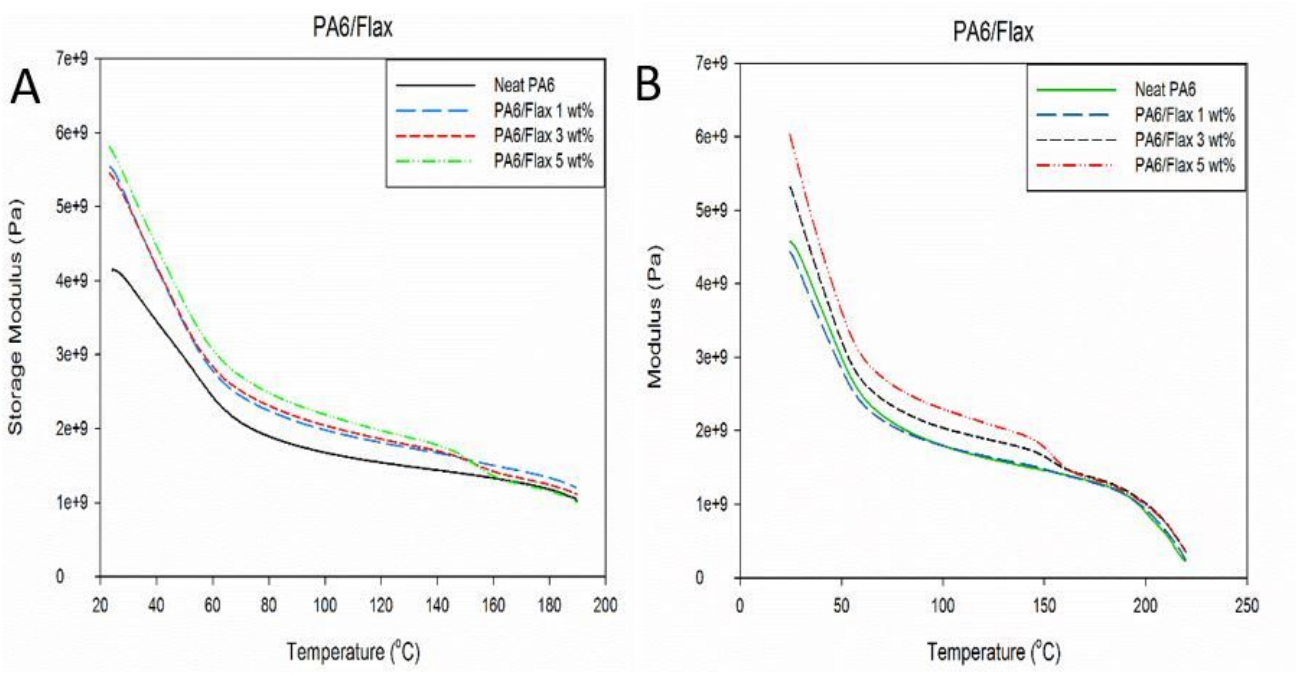

Figure 2

a.) Shows the storage modulus vs temperature and b is modulus Vs temperature of neat PA6 and PA6/Flax Linum composites

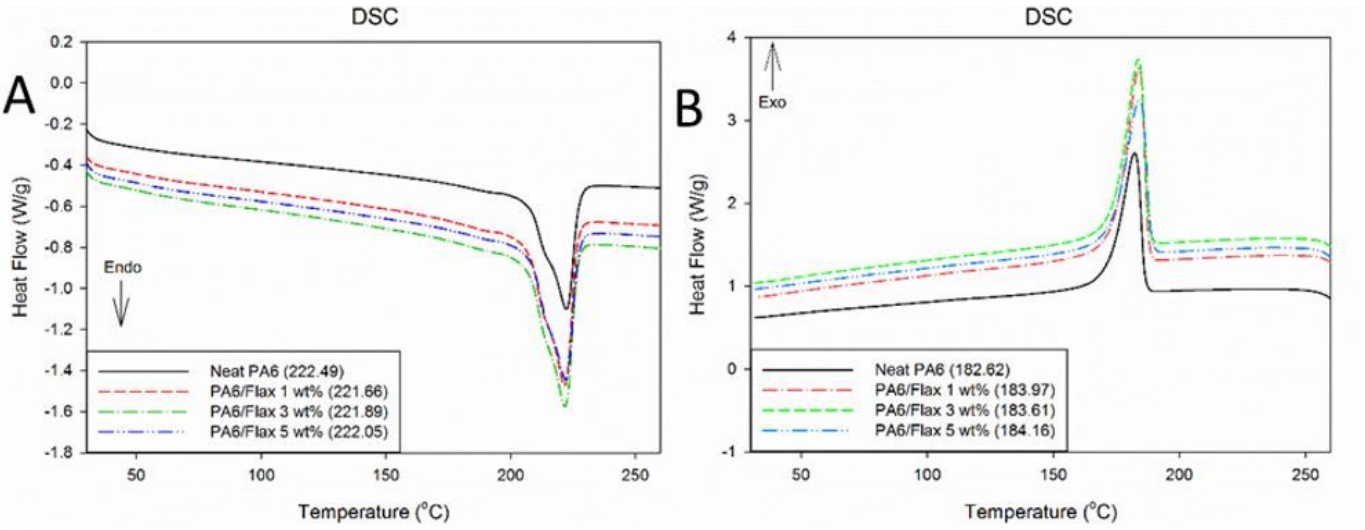

Figure 3

DSC curves of PA6 and PA6/Flax Linum for crystallization (a) and melting (b)

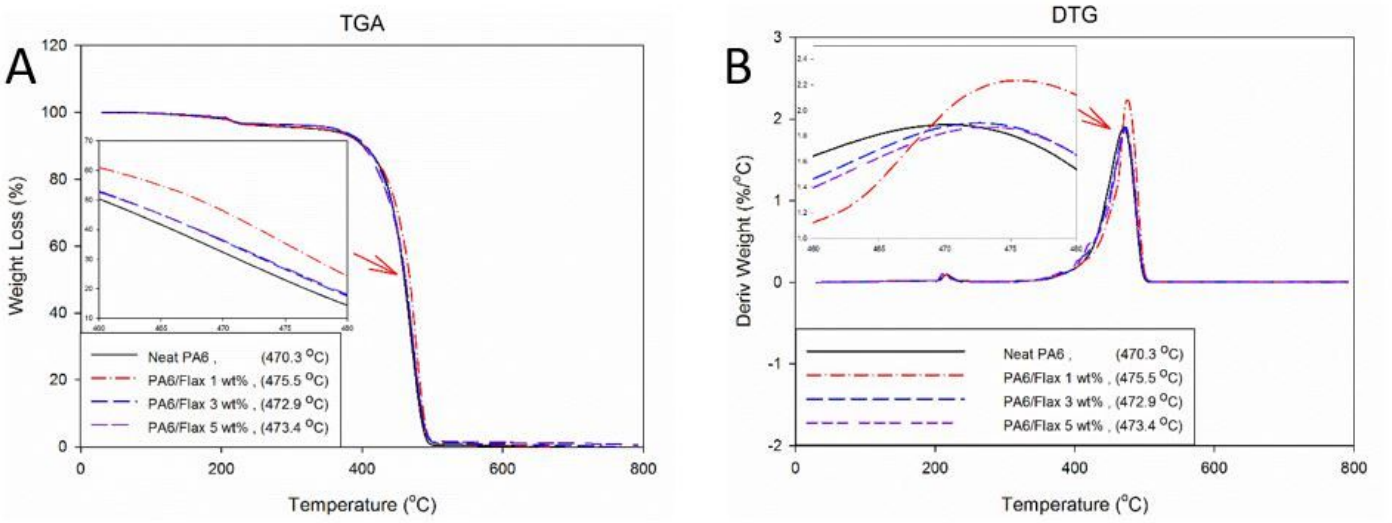

Figure 4

a) TGA curve and b) DTG analysis of PA6/Flax

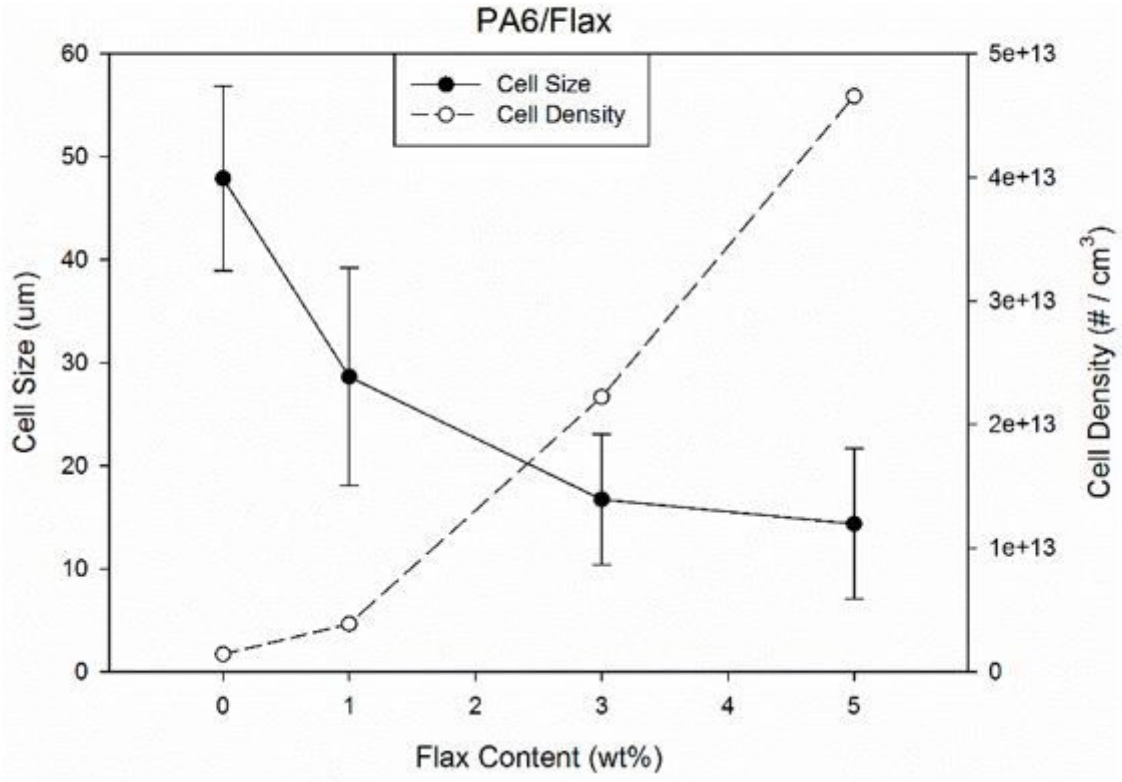

Figure 5

illustration of impact of flax on PA6 cell size and density

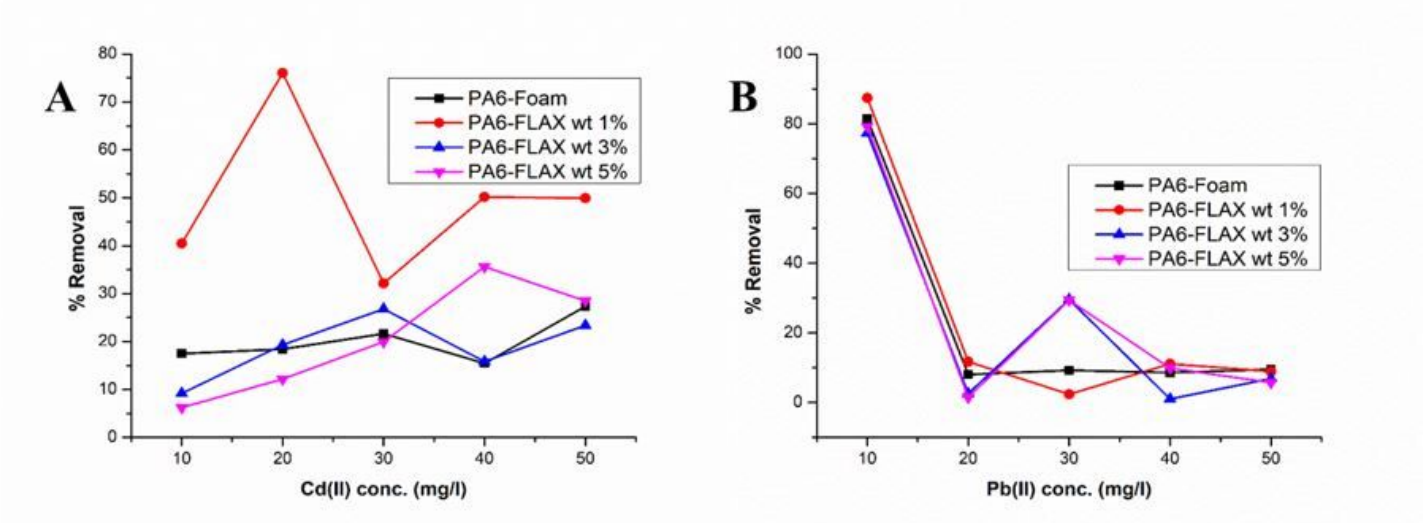

Figure 6

Effect of initial concentration for adsorption Cd(II) [A] and Pb(II) [B] using PA6-Flax Linum composite (0.5g dosage of PA6, PA6-Flax Linum Wt%)

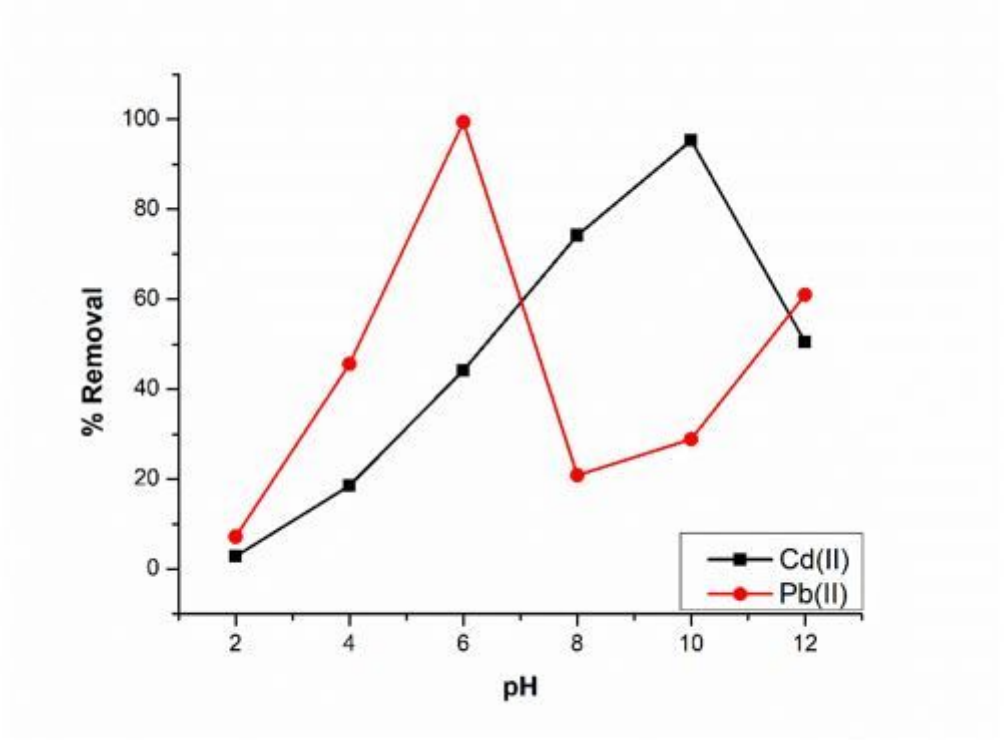

Figure 7

Effect of pH for adsorption Cd(II) and Pb(II) at optimum concentration (20, 10 respectively) using PA6-Flax Linum composite

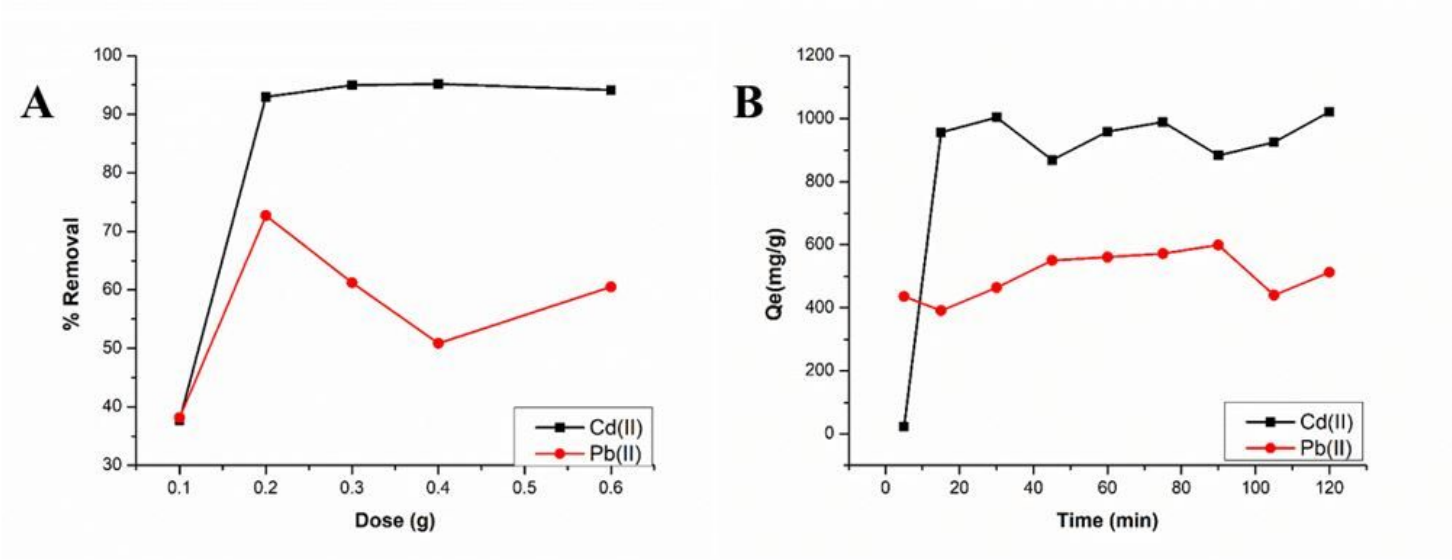

Figure 8

a.) Effect of dosage for adsorption Cd (II) and Pb (II) using PA6-Flax Linum composite and b.) : Effect of time in capacity adsorption for remediation Cd(II) and Pb(II) using PA6-Flax Linum wt 1% composite

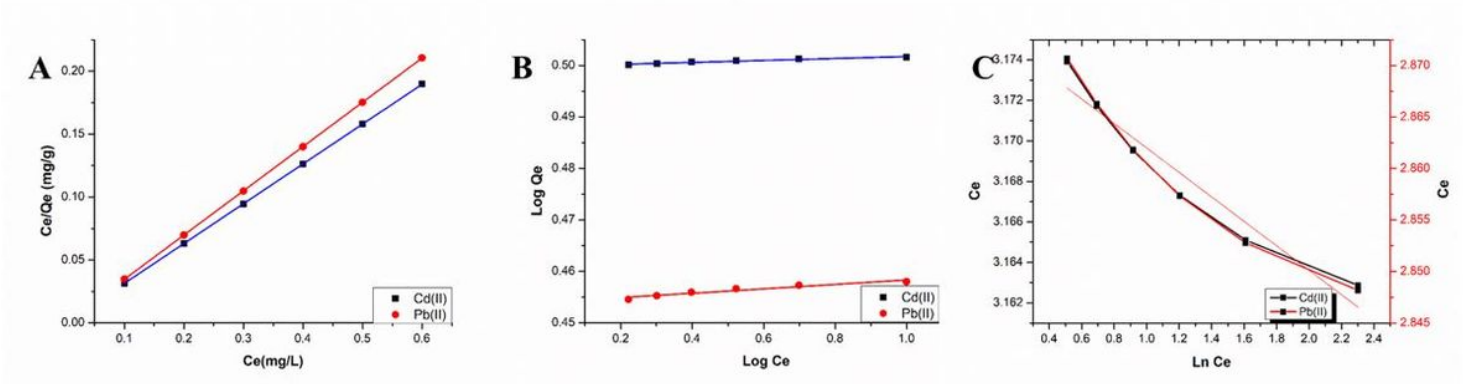

Figure 9

Linearized fits for Langmuir isotherm 10 mg/l of Pb(II) and 20 mg/l of Cd(II) of by PA6/Flax 1wt% , b) Linearized fits for Freundlich isotherm 10 mg/l of Pb (II) and 20 mg/l of Cd(II), of PA6/Flax 1wt% composite, C) Linearized fits for Temkins isotherm 10 mg/l of Pb (II) and 20 mg/l of Cd(II), of PA6/Flax 1wt% composite

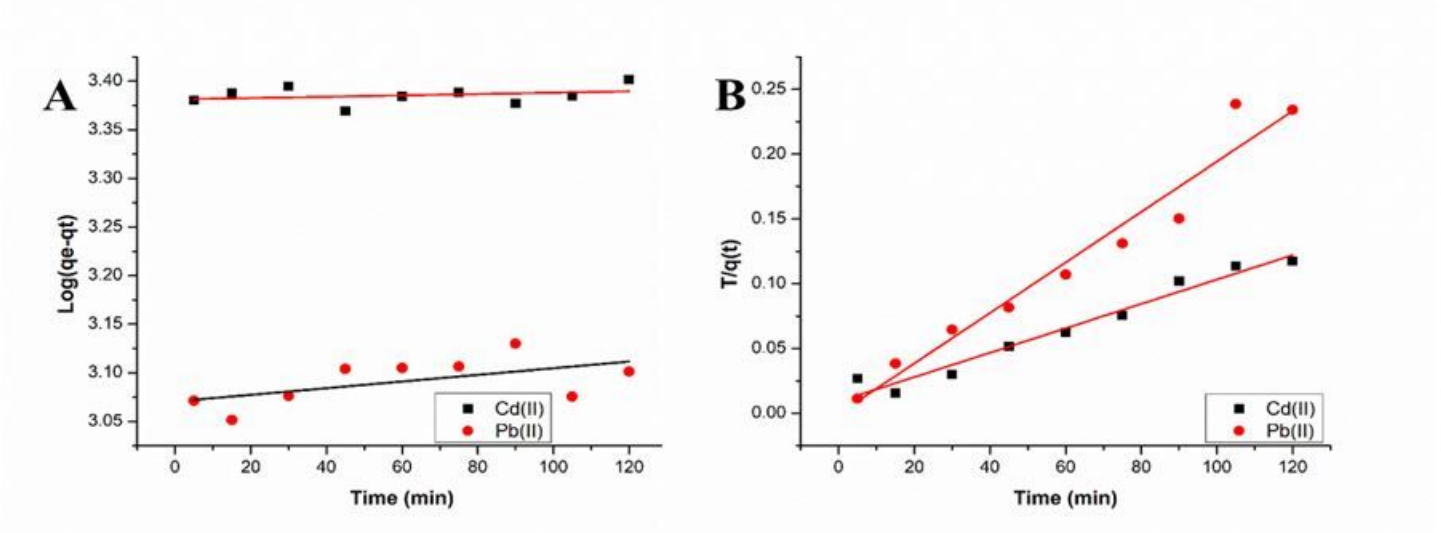

Figure 10

Linearized fits for pseudo 1st order (A) of PA6/Flax, Linearized fits for 2nd order (B) of PA6/Flax composite

Supplementary Files

This is a list of supplementary files associated with this preprint. Click to download.

- S1.jpg